

National Aeronautics and Space Administration  
Headquarters  
Washington, D. C.

15 January 1966

GCA CORPORATION  
GCA TECHNOLOGY DIVISION  
Bedford, Massachusetts

PLANETARY METEOROLOGY  
Quarterly Progress Report No. 3  
Covering the Period  
1 October 1965 - 31 December 1965  
Contract No. NASW-1227

## TABLE OF CONTENTS

<u>Section</u>	<u>Title</u>	<u>Page</u>
1	INTRODUCTION	1
2	THE SEASONAL CLIMATOLOGY OF MARS	3
	2.1 Introduction	3
	2.2 Input Parameters and Method of Calculation	3
	2.3 Seasonal Climatology Results	7
3	ATMOSPHERIC CIRCULATION ON MARS	15
4	INTERHEMISPHERIC TRANSPORT OF WATER VAPOR AND THE MARTIAN ICE CAPS	24
5	ADMINISTRATIVE NOTES	26
	REFERENCES	27

## SECTION 1

### INTRODUCTION

During the past quarter, work has continued on various phases of our Planetary Meteorology research. The results of calculations of the average surface and atmospheric temperatures as functions of season and latitude are presented and discussed in Section II, The Seasonal Climatology of Mars. The computed temperatures are based upon a radiative equilibrium model in which it is assumed that the surface and atmosphere are both in radiative equilibrium at any time and location. A contract Technical Report will be prepared on this work.

The two-level circulation model described in Quarterly Report No. 2 is used to re-compute the mean zonal and meridional velocities, and pole-to-equator temperature difference on Mars. An atmospheric model based upon a surface pressure of 5 mb is used as opposed to the 25 mb surface pressure model used in the previous computations. The results of these calculations are discussed in Section III, Atmospheric Circulation on Mars. A contract Technical Report is being prepared on this work.

The large-scale eddy diffusion model for the interhemispheric transport of water vapor on Mars is being used to derive rates of meridional transport of water vapor. These rates are being compared to the observed rate of

meridional movement of the "wave of darkening." The objective of this comparison is to determine if there is an appropriate value of the large-scale atmospheric eddy diffusion coefficient that can explain the observed speed of propagation of the "wave of darkening." Progress on this work is summarized in Section III, Interhemispheric Transport of Water Vapor and the Martian Ice Caps.

## SECTION 2

### THE SEASONAL CLIMATOLOGY OF MARS

#### 2.1 INTRODUCTION

Our study of the seasonal climatology of Mars has been based on two simple theoretical models which are used to determine the latitudinal and seasonal variation of surface and mean atmospheric temperatures. In this section of the report, we present results of calculations, based on the radiative equilibrium model.

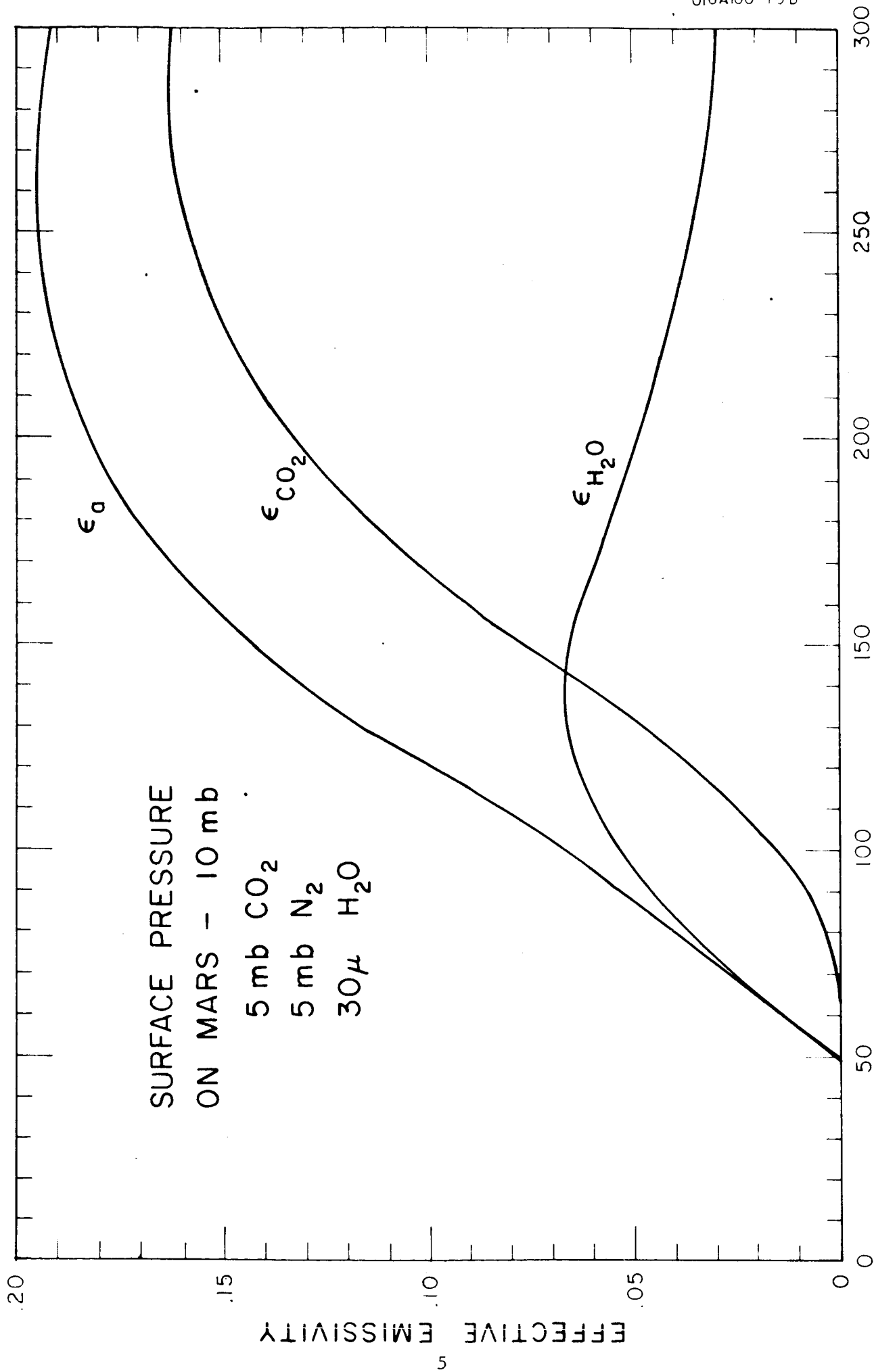
#### 2.2 INPUT PARAMETERS AND METHOD OF CALCULATION

In the second quarterly project report, it was shown that the temperature climate on Mars was insensitive to the choice of atmospheric composition and surface pressure. As a result, an atmosphere whose surface pressure is 10 mb, consisting of 5 mb  $\text{CO}_2$  and 5 mb  $\text{N}_2$ , seemed to be a reasonable choice for this study. A water vapor amount of 30 precipitable microns  $\text{H}_2\text{O}$  was also assumed. For this atmosphere, the normal beam transmission to solar radiation is 0.989, or, stating the result in another way, only 1.1 percent of the solar radiation is absorbed by the atmosphere before reaching the surface for normal incidence. Of course, the amount of solar radiation absorbed will vary with different slant paths of the sun's rays through the atmosphere.

Other input parameters that are important in the calculations include the effective emissivities for carbon dioxide and water vapor to long-wave radiation. It was also shown in the last quarterly report that these effective emissivities vary with the absolute temperature of the emitting gas, a result which is due to the changing weighting distribution of the Planck function with temperature. For the range of temperatures found on Mars, the effective emissivity of the atmosphere varies directly as the temperature.

Computed variations of effective emissivity with temperature for carbon dioxide and water vapor, are shown in Figure 1. The effective emissivity for carbon dioxide,  $\epsilon_{\text{CO}_2}$ , increases steadily with temperature, and then reaches a maximum value, corresponding to the shift of the Planck function maxima to wave numbers in the  $\text{CO}_2$  absorption band. In the case of the effective emissivity for water vapor,  $\epsilon_{\text{H}_2\text{O}}$ , the values increase and then decrease, corresponding to the shift of the Planck function maxima from wave numbers in the rotational band to higher wave numbers between the rotational and  $6.3\mu$  bands. The effective emissivity for the atmosphere,  $\epsilon_a$  in Figure 1, is the sum of the curves for  $\epsilon_{\text{H}_2\text{O}}$  and  $\epsilon_{\text{CO}_2}$ , since there is no overlap of the absorption bands for the low atmospheric pressures found on Mars.

A curve similar to the one for  $\epsilon_a$  holds for the effective absorptivity,  $\alpha_a$ , of the atmosphere to long-wave radiation from the surface. For a given temperature in Figure 1,  $\alpha_a$  is equal to  $\epsilon_a$ . It must be remembered,



Variation of the effective emissivity for carbon dioxide,  $\epsilon_{CO_2}$ , with atmospheric temperature.

The sum of these curves is the effective emissivity,  $\epsilon_a$ .

however, that  $\alpha_a$  is a function of the surface temperature and  $\epsilon_a$  is a function of the atmospheric temperature. Normally  $\alpha_a$  is not equal to  $\epsilon_a$  for a given calculation of the radiative heat budget.

The calculation of atmospheric and surface temperature is complicated by the fact that the atmospheric absorptivity and emissivity are dependent variables, and are functions, themselves, of the temperatures to be calculated. Thus, for example, the algebraic solution to determine the atmospheric temperature is not readily apparent for given values of solar energy input, and cannot be determined from a single calculation using the energy balance equations.

However, an exact solution to the equations can be found, using the method of successive approximations in the computer (trial and error method). The process of iteration is as follows: Values of atmospheric absorptivity and emissivity are assumed as an approximation to the exact values. Then the surface and atmospheric temperatures are computed using the energy balance equations. These computed temperatures establish new values of absorptivity and emissivity, which, in turn, yield better approximations to the equilibrium temperatures, etc. This iteration process converges rapidly to the exact solution of the energy balance equations. For example, the temperatures are accurate to within one degree of the exact solution after four or five iterations in the computer.



### 2.3 SEASONAL CLIMATOLOGY RESULTS

Calculation of the latitudinal distribution of surface and atmospheric temperatures was carried out at ten-day intervals for the entire Martian year. These results give some indication of the variations of temperatures within a seasonal period. In addition to the temperature calculations at ten-day intervals, the average input of solar energy at the top of the atmosphere and at the surface was computed for each season and for the annual mean. From these results it is possible to compute representative, seasonal average surface and atmospheric temperatures as well as the mean annual temperatures.

The graphs in Figure 2 show the latitudinal variation of the average daily insolation on Mars at the top of the atmosphere for the different seasons and for the annual mean. Units are in  $\text{cal cm}^{-2} \text{ day}^{-1}$  where a day represents one Martian day, 1477 minutes. In these calculations, the seasons represent time periods of the Martian year which are centered about the equinoxes and solstices. Thus, Summer is the warm season, Winter is the cold season, and Spring and Fall represent the transitional seasons between the extremes. Such a division of seasons has more meaning in a meteorological and climatological sense than the astronomical division of the seasons which is taken to be the periods between the solstices and equinoxes.

Curves for the variation of insolation at the surface of Mars are similar to those shown in Figure 2 except that they are slightly reduced

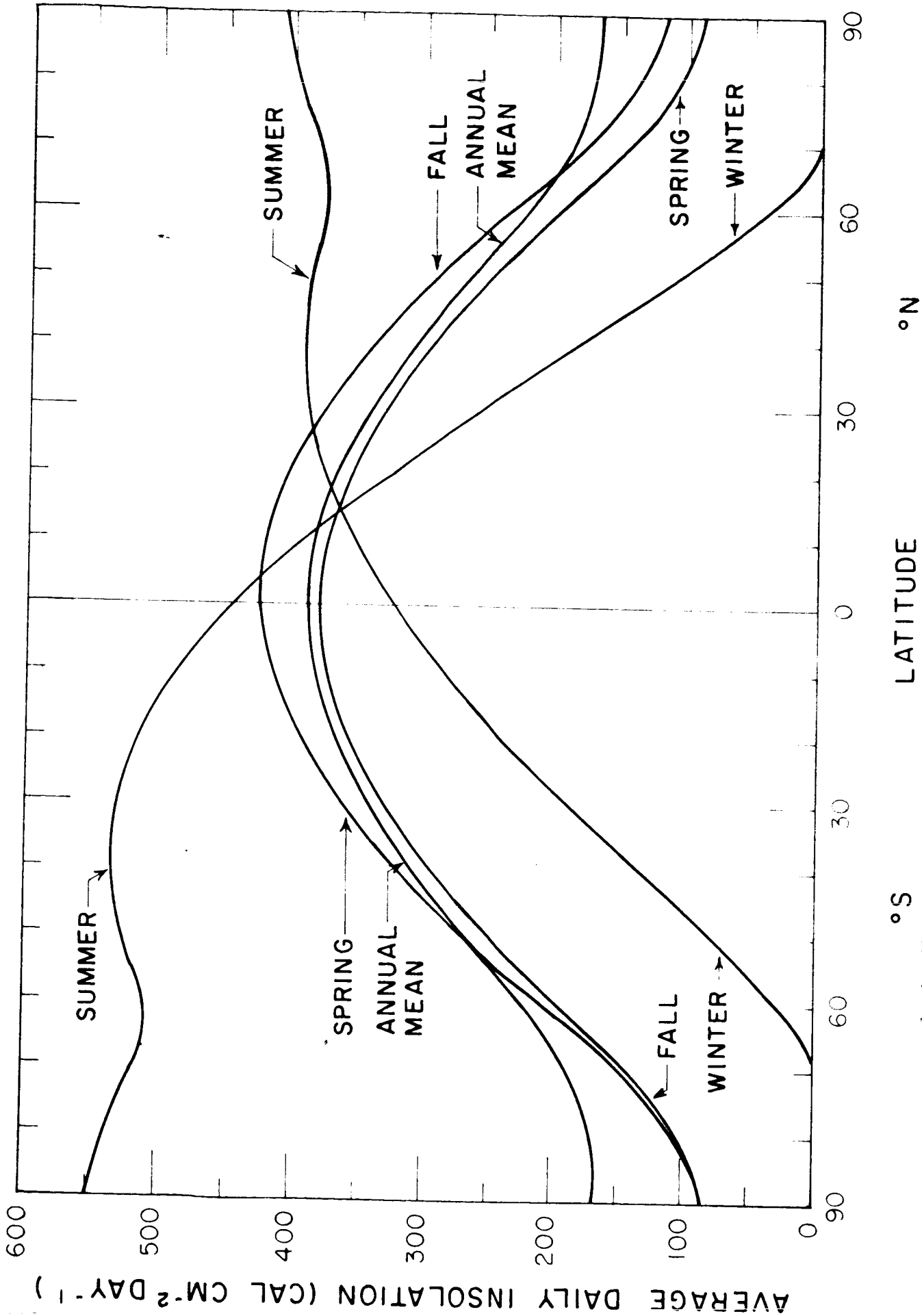


Figure 2. The latitudinal variation of the average daily insolation on Mars at the top of the atmosphere. The spring and fall seasons and the summer and winter seasons represent periods of the Martian year which are centered about the equinoxes and solstices, respectively. A solar constant of  $2.00 \text{ cal. cm}^{-2} \text{ min}^{-1}$  is assumed in the calculations.

in magnitude. On the average for the annual mean, about 2.0 percent of the solar radiation is absorbed by the atmosphere before reaching the surface. This absorption varies with latitude, being about 1.7 percent at the equator and 3.8 percent at the poles. For long slant paths through the atmosphere, the absorption of solar radiation by the atmosphere can be as much as 13 percent of the incident energy.

The graphs in Figures 3, 4, and 5 summarize the calculated results of the seasonal climatology on Mars using the radiative equilibrium model. The contrasting seasons of Winter and Summer are compared in Figure 3, the latitudinal variation of surface and atmospheric temperatures for the Spring and Fall seasons are shown in Figure 4, and the summary of the mean annual temperatures is indicated in Figure 5.

Each set of curves for the seasons has a discontinuity at latitudes ranging from  $20^{\circ}$  to  $60^{\circ}$ . These discontinuities represent the equatorward extension of the polar ice caps and are based on the dew point temperature of the atmosphere at the surface. Assuming that the 30 microns of precipitable water vapor in the atmosphere are evenly mixed, the dew point at the surface for a 10 mb surface pressure is  $202^{\circ}\text{K}$ . Thus, in the calculations, if the computed surface temperature was below  $202^{\circ}\text{K}$ , it was assumed that the ice cap had formed and that the albedo of the surface increased from 31 percent to 45 percent, the approximate albedo of dirty snow. As a result, the computed values of surface and atmospheric temperatures decrease with the albedo increase, thus, producing a discontinuity in the temperature profiles.

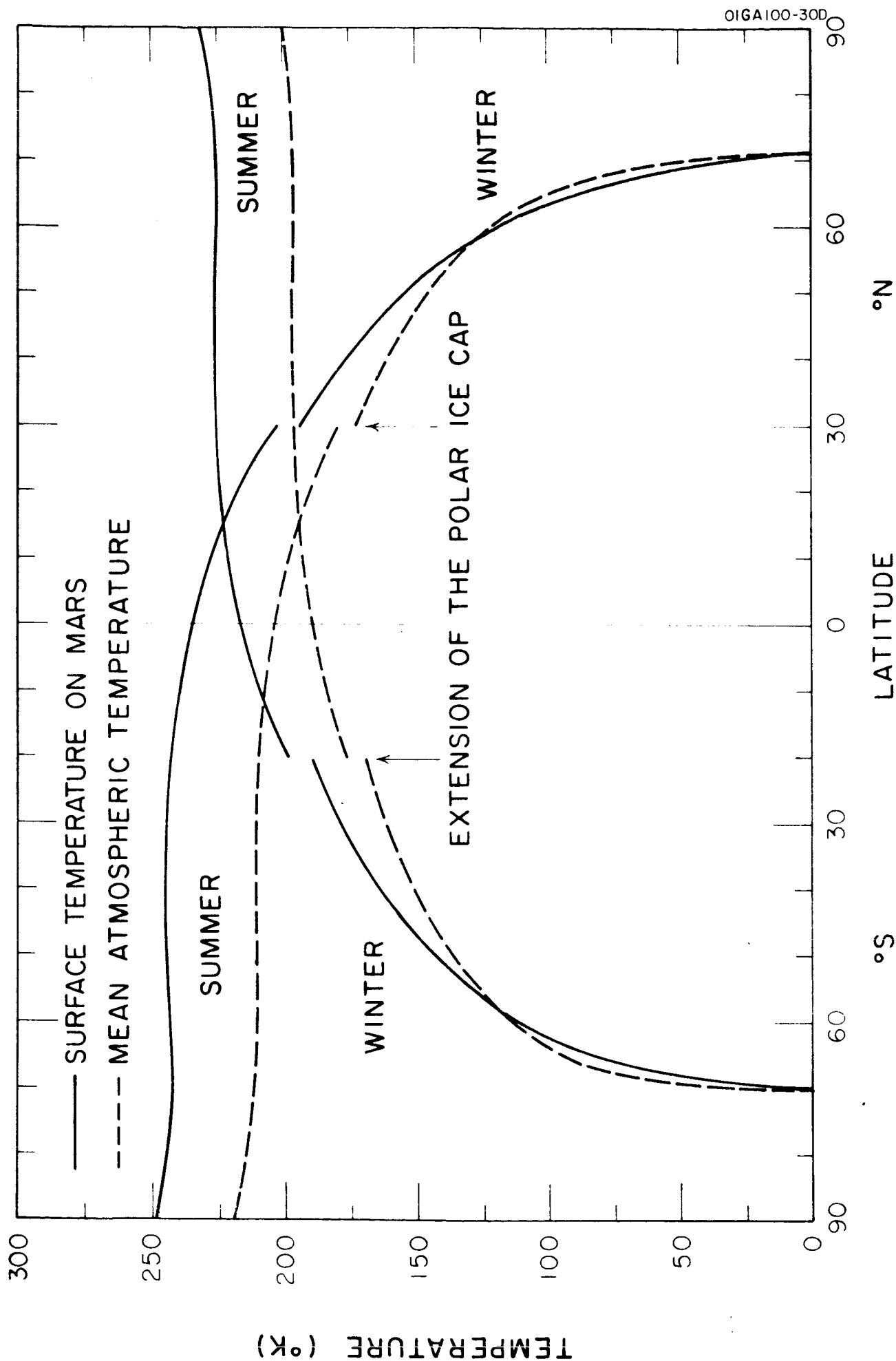


Figure 3. Latitudinal variation of the average surface and atmospheric temperatures on Mars for the summer and winter seasons. The equatorward extension of the polar ice cap is indicated by the discontinuity in the lines.

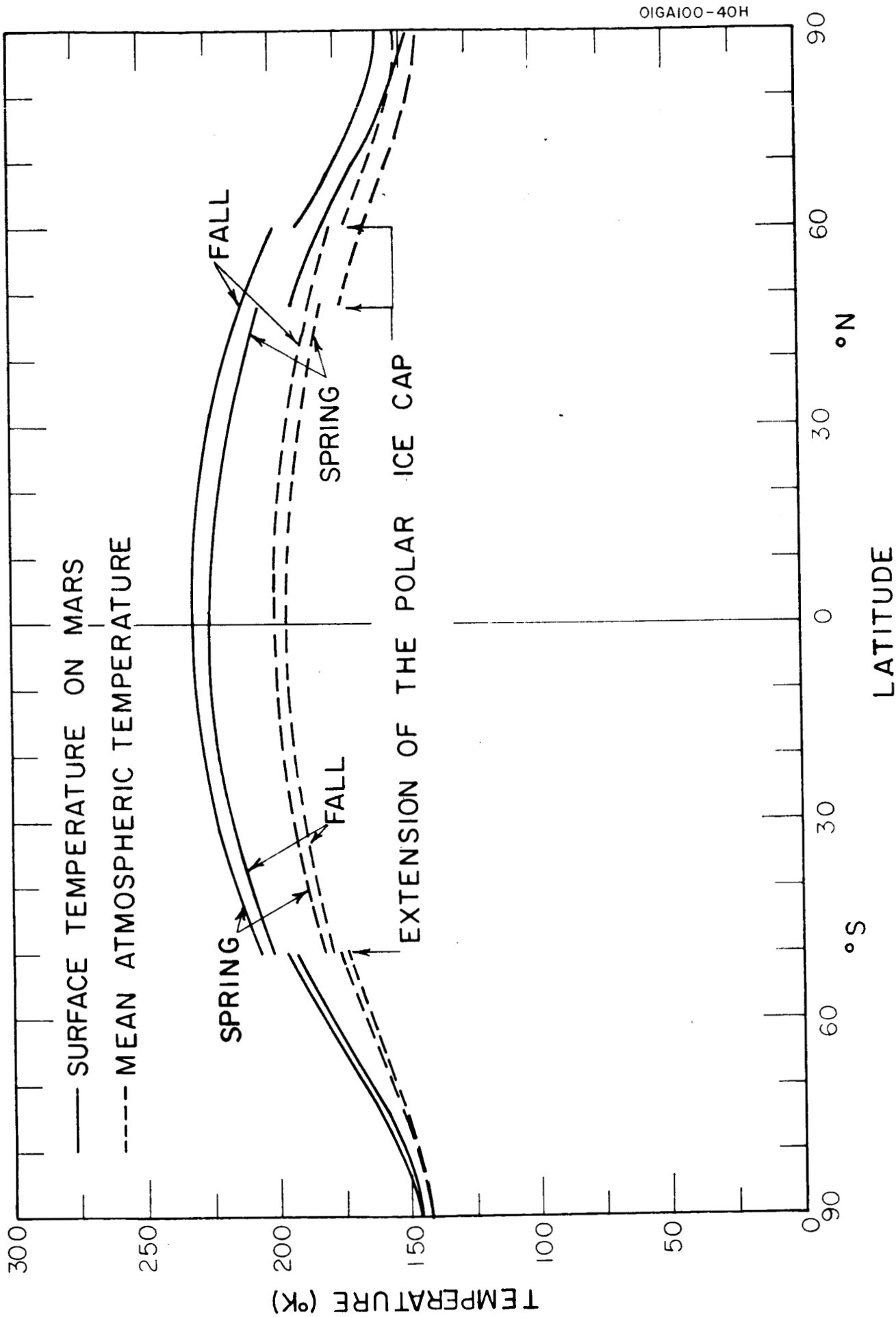


Figure 4. Latitudinal variation of the average surface and atmospheric temperatures on Mars for the spring and fall seasons. The equatorward extension of the polar ice cap is indicated by the discontinuity of the lines.

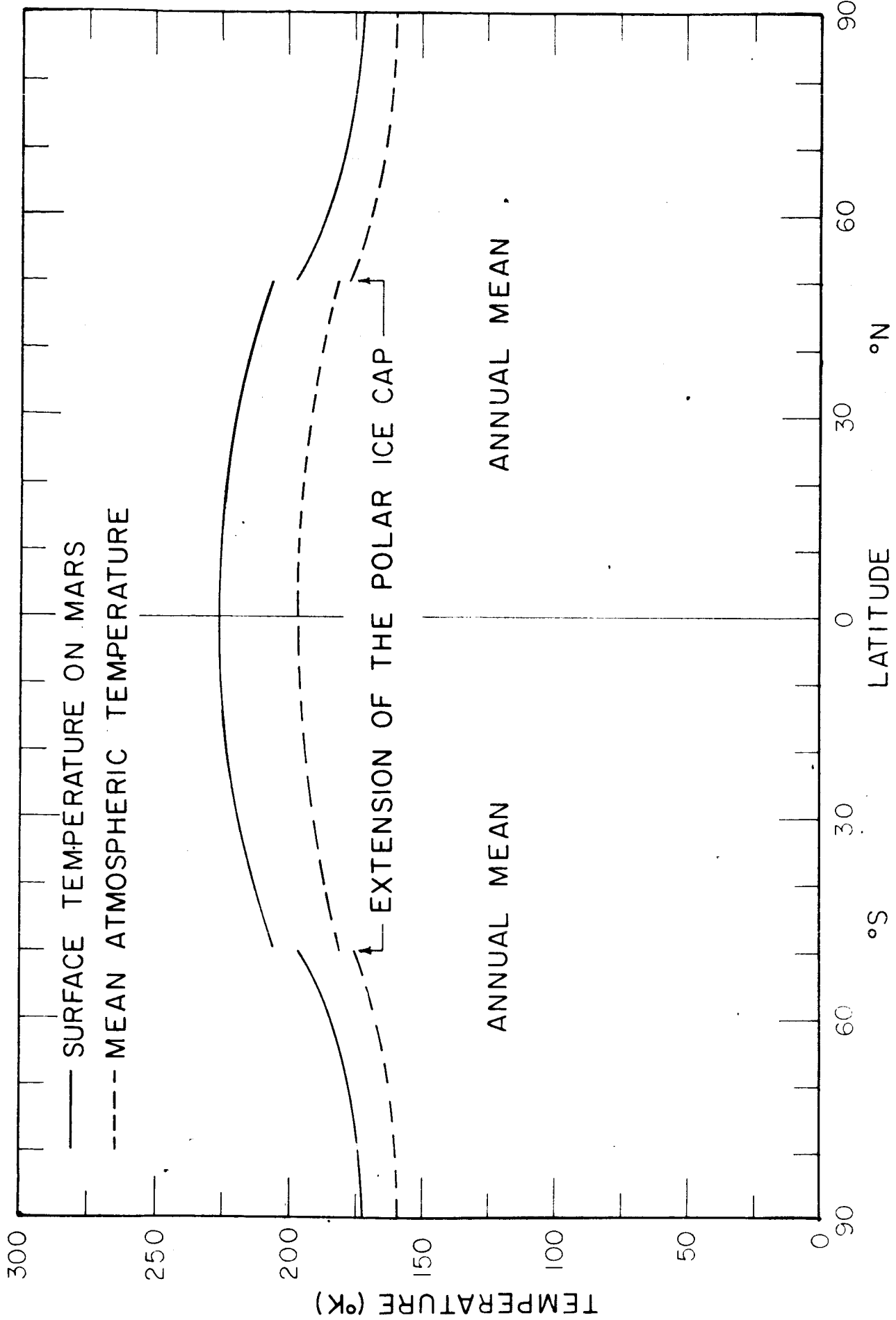


Figure 5. Latitudinal variation of the average surface and atmospheric temperatures on Mars for the annual mean. The discontinuity in the lines indicates the equatorward extension of the polar ice cap.

Some of the salient features of the seasonal climatology on Mars are evident from an analysis of the temperature profiles. In Figure 3, it is evident that the summer poles in both hemispheres have the highest average surface temperature, the south pole temperature ( $248^{\circ}\text{K}$ ) being somewhat warmer than the north pole temperature ( $230^{\circ}\text{K}$ ). The mean atmospheric temperatures during a summer run about  $30^{\circ}\text{C}$  colder than the computed surface temperatures, and the pole to equator temperature difference in each hemisphere is quite small during summer, about  $12$  to  $14^{\circ}\text{C}$ .

In contrast to the summer seasons, the winter seasons show a marked decrease in temperatures at latitudes poleward of the equator. The curves in Figure 3 indicate that the difference between the surface and atmospheric temperatures decreases with increasing latitude, and, at latitudes greater than  $58^{\circ}$ , the mean atmospheric temperature is larger than the surface temperature. Such a temperature configuration as this suggests a strong temperature inversion at the surface which is indeed the case on Earth at high latitudes during winter. Two factors contribute to these warmer atmospheric temperatures at high latitudes: 1) greater absorption of solar radiation by the atmosphere relative to surface absorption because of the long slant path through the atmosphere, and 2) the effective emissivity of the atmosphere decrease with temperature.

In Figure 4, the Spring and Fall seasons in both hemispheres indicate similar temperature profiles. As in the case of the Summer seasons, the temperature difference between the surface and atmosphere is about  $30^{\circ}\text{C}$

at the equator. This difference decreases with increasing latitude, diminishing to about  $6.5^{\circ}\text{C}$  at the poles. The temperature profiles indicating Spring in the southern hemisphere and Fall in the northern hemisphere are somewhat warmer than the profiles for the opposing seasons, because the planet is closer to the sun at this time.

The profiles in Figure 5 indicate the mean annual temperature climate on Mars. Probably the most pronounced feature of these results is the symmetry of temperatures about the equatorial region, the northern hemisphere being slightly warmer due to the greater amount of insolation received there in the annual mean. Surface and atmospheric temperatures at the equator are  $226.1^{\circ}\text{K}$  and  $196.3^{\circ}\text{K}$ , respectively, and decrease to about  $173.3^{\circ}\text{K}$  and  $160.5^{\circ}\text{K}$  at the poles.

The effect of the atmospheric transport of heat on the temperature climate, computed from the radiative equilibrium model, would be a decrease in the temperature gradients with latitude, especially the atmospheric temperature gradient. This effect would be quite evident during the winter seasons at high latitudes during the polar night. When using the radiative equilibrium model, the computed temperatures are zero because there is no solar input of energy. With heat transport into these latitudes, the temperature will increase to between  $50^{\circ}\text{K}$  and  $100^{\circ}\text{K}$ , depending on the latitude. In the case of the Summer seasons, the effect of heat transport will have hardly any effect on the temperature gradient and will cause only a small lowering of the temperature magnitudes. The effect produced by heat transport for the Spring and Fall seasons will be somewhat larger than the Summer season.



### SECTION 3

#### ATMOSPHERIC CIRCULATION ON MARS

In Quarterly Progress Report No. 2, a two-level circulation model was described and applied to Mars. Mean zonal and meridional velocities, and the pole-to-equator temperature difference were computed for a 25 mb surface pressure model, in which the atmosphere is composed largely of nitrogen. The recent occultation experiment on Mariner IV (Kliore et al, 1965) suggests that the Martian surface pressure is much lower than 25 mb -  $\sim 5$  mb. Therefore, the calculations were repeated for a surface pressure model of 5 mb, in which the atmosphere is assumed to be 100 percent carbon dioxide. In the model, the internal friction is related to the value of the pressure, and, hence, one can expect the velocities to change as the value of the surface pressure is varied. The new assumed composition changes the value of the gas constant, which also affects the final wind velocities. In addition to the changes in assumed surface pressure and composition, the value of the infrared absorptivity of the atmosphere is changed to reflect the results obtained in our studies of the seasonal climatology of Mars (see Quarterly Progress Report No. 2). These changes lead to a new set of values for the mean zonal and meridional winds and the pole-to-equator temperature gradient on Mars. A sample of the results obtained is discussed below.

For a surface pressure of 5 mb, specific heat at constant pressure of  $0.203 \text{ cal gm}^{-1} \text{ deg}^{-1}$ , gas constant of  $1.89 \times 10^6 \text{ cm}^2 \text{ sec}^{-2} \text{ deg}^{-1}$ , infrared absorptivity of 0.18, mean temperature of the atmosphere of  $185^\circ\text{K}$ , radius of Mars of  $3.4 \times 10^8 \text{ cm}$ , gravitational acceleration of Mars of  $373 \text{ cm sec}^{-2}$ , Coriolis parameter of  $0.9 \times 10^{-4} \text{ sec}^{-1}$ , lateral eddy viscosity of  $10^{10} \text{ cm}^2 \text{ sec}^{-1}$  and coefficients of vertical eddy viscosity of 50 to  $200 \text{ gm cm}^{-1} \text{ sec}^{-1}$ , we obtain the mean zonal and meridional wind velocities at various levels as shown in Figures 6 and 7.

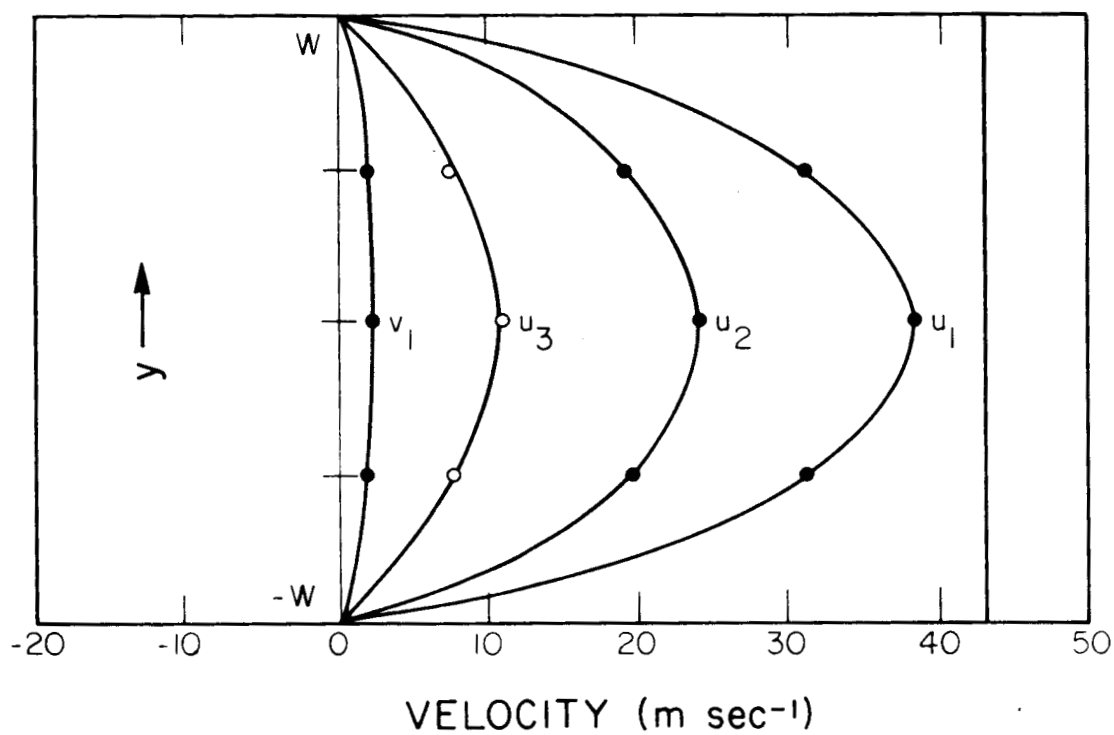
For the non-viscous cases, the mean zonal winds at level 1,  $\bar{u}_1$ , are shown by straight lines in the extreme right in Figure 6. In these cases, the mean zonal wind is simply

$$\bar{u}_1 = \frac{3 R T_m}{8 a f_o} ,$$

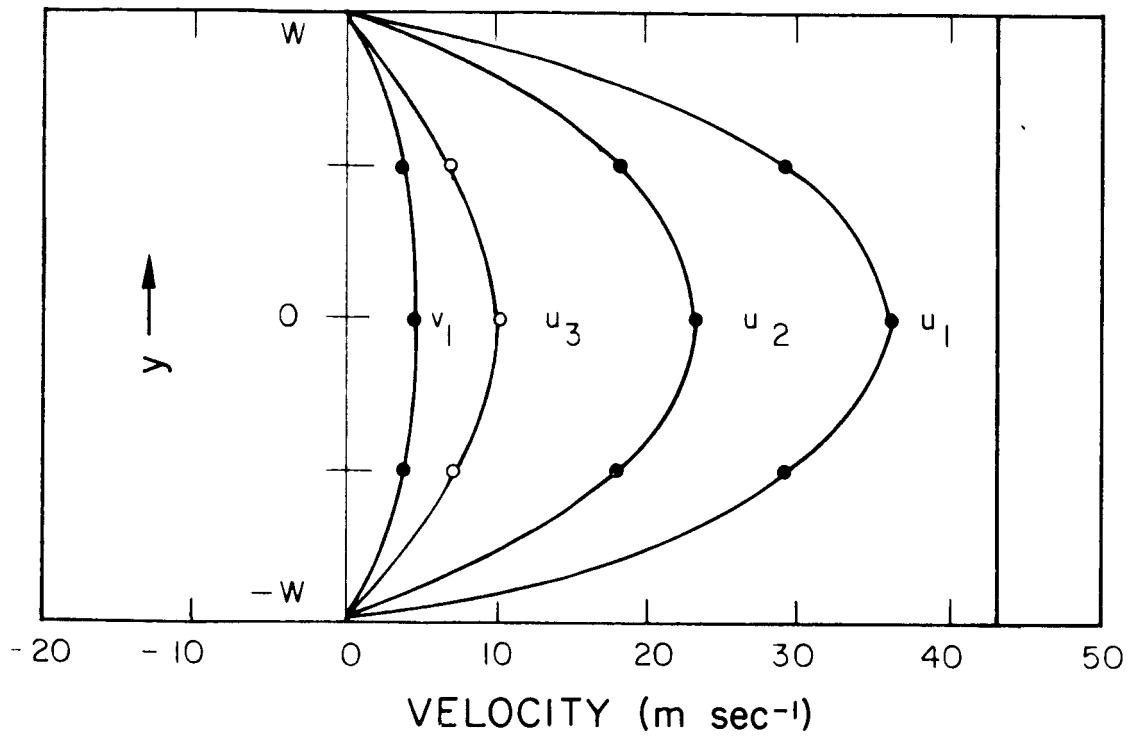
where  $R$  is the gas constant,  $T_m$  is the mean atmospheric temperature,  $a$  is the radius of the planet, and  $f_o$  is the mean Coriolis parameter. It is seen that  $\bar{u}_1$  is proportional to the gas constant,  $R$ . For 100 percent  $\text{CO}_2$  content,  $R$  is about  $1.89 \times 10^6 \text{ cm}^2 \text{ sec}^{-2} \text{ deg}^{-1}$  and is only about 2/3 of the gas constant for air in the terrestrial atmosphere. Since the mean atmospheric temperature of the Martian atmosphere is about  $180^\circ\text{K}$ , less than that on Earth, the product of  $R$  and  $T_m$  will lead to a smaller wind velocity than on Earth. However,  $\bar{u}_1$  is inversely proportional to the radius of the planet. Since the radius of Mars is about one half of the Earth's radius, the mean zonal winds on Mars are slightly higher than on Earth. If the lateral eddy viscosity is taken into account, the

Figure 6. Mean wind velocities at different levels for lateral eddy viscosity  $A$  of  $10^{10} \text{ cm}^2 \text{ sec}^{-1}$  and vertical coefficients of eddy viscosity  $\mu$  of 50, 100, and 200  $\text{gm cm}^{-1} \text{ sec}^{-1}$ .  $U_1$ ,  $U_2$ , and  $U_3$  are mean zonal winds at levels 1, 2, and 3, respectively;  $V_1$  is the mean meridional wind at level 1.

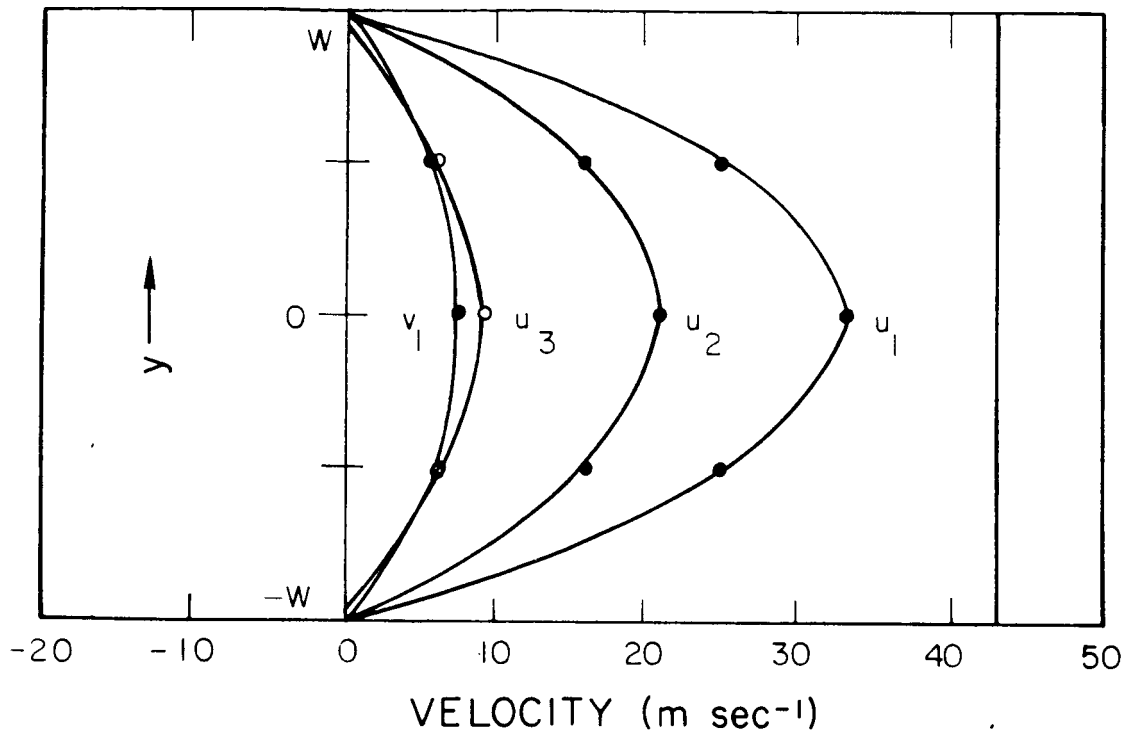
OIGA97 - 20F



(a) Case of  $\mu = 50 \text{ gm cm}^{-1} \text{ sec}^{-1}$



(b) Case of  $\mu = 100 \text{ gm cm}^{-1} \text{ sec}^{-1}$ .



(c) Case of  $\mu = 200 \text{ gm cm}^{-1} \text{ sec}^{-1}$ .

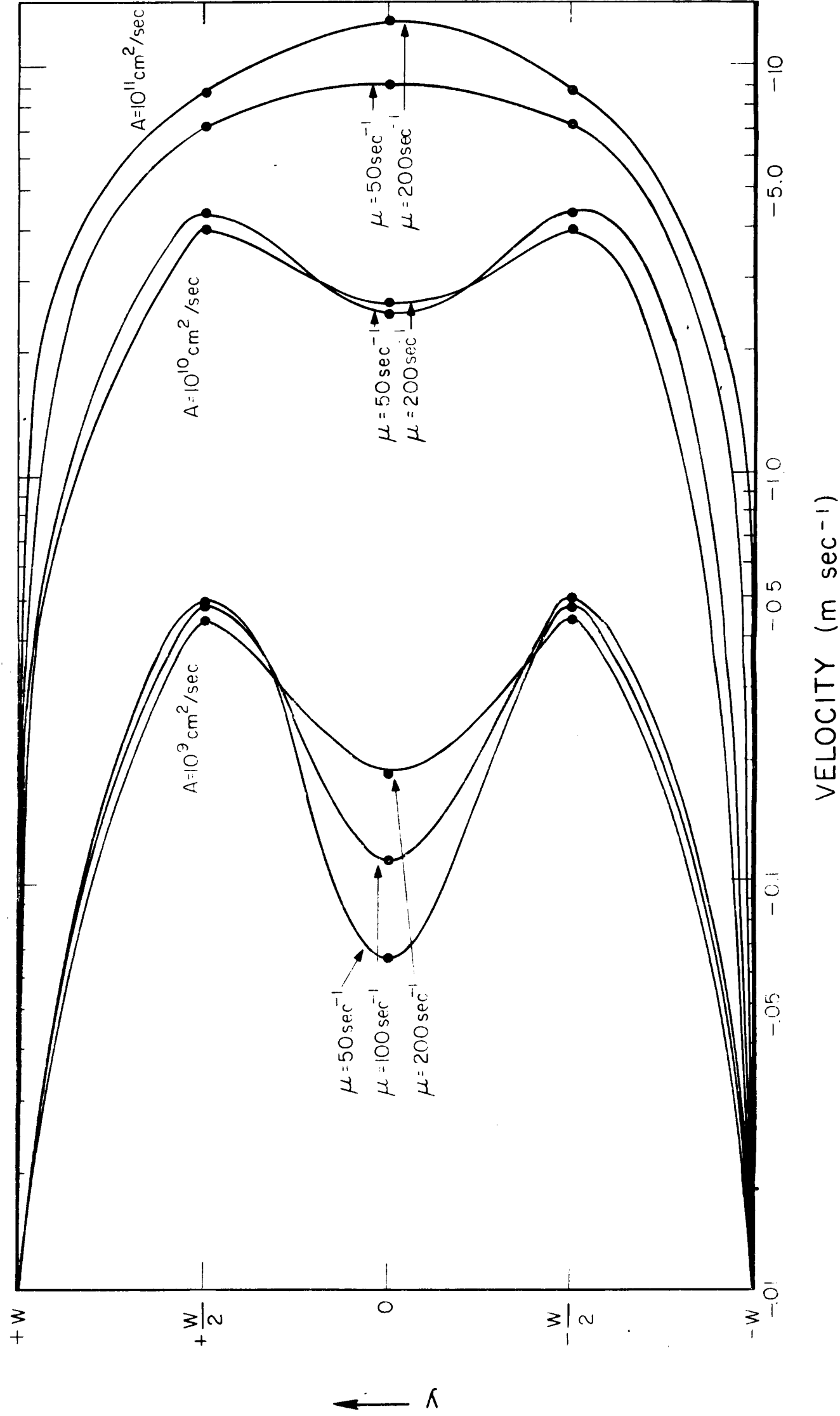


Figure 7. Mean surface wind velocities for lateral eddy viscosity  $A$  of  $10^{10} \text{ cm}^2 \text{ sec}^{-1}$  and vertical coefficients of eddy viscosity as indicated.

estimated magnitude of the zonal wind velocity would be somewhat reduced, depending upon the magnitude of the lateral eddy viscosity chosen. Based upon the empirical and theoretical studies by Richardson and Oboukhov (see Gandii, 1955) on the relation between the lateral eddy viscosity and the scale of motion of a system, the lateral eddy viscosity, A, may be written as

$$A \approx 10^{-2} L^{4/3} \text{ m}^2 \text{ sec}^{-1} .$$

For the scale of eddies of the general circulation in the terrestrial atmosphere

$$L \approx 2 \times 10^6 \text{ m}$$

and, hence,  $A \approx 2.5 \times 10^{10} \text{ cm}^2 \text{ sec}^{-1}$ . This value was used by Adem (1962) with some success. If  $A = 10^{10} \text{ cm}^2 \text{ sec}^{-1}$  is used in our model to compute the wind velocity in the Earth's atmosphere, the computed values at levels 1 and 3 are

$$\bar{u}_1 = 33 \text{ m sec}^{-1} \quad \text{and} \quad \bar{u}_3 = 10 \text{ m sec}^{-1}$$

which are in reasonable agreement with the observed values. Therefore,  $A = 10^{10} \text{ cm}^2 \text{ sec}^{-1}$  is probably a proper value for the Earth's atmosphere. What is the most probable value of A for Mars? No one really knows. A reasonable estimate might be a value similar to that in the Earth's atmosphere —  $A = 10^{10} \text{ cm}^2 \text{ sec}^{-1}$ . Further justification for a value of  $A = 10^{10} \text{ cm}^2 \text{ sec}^{-1}$  for Mars comes from a recent study (see Quarterly Report No. 2) of the value of the large scale eddy diffusion coefficient that is required to transport water vapor from the melting polar cap to the forming polar cap on Mars.

As to the coefficient of vertical eddy viscosity,  $\mu$ , the average value for Earth is about  $100 \text{ gm cm}^{-1} \text{ sec}^{-1}$ . The same value of  $\mu$  is assumed in the calculation for Mars' atmosphere.

The computed meridional wind velocities for Mars are on the average about one order of magnitude higher than those of the Earth. Since the magnitude of the meridional wind velocity is almost inversely proportional to surface pressure, the meridional wind velocity on a planet having a small surface pressure will be larger. It is highly probable that the high percentage of meridional cloud movements at low latitudes on Mars (Gifford, 1965; Tang, 1965) is directly associated with the relatively strong mean meridional wind velocity and indirectly with the low value of the surface pressure on Mars.

The computed pole-to-equator temperature differences for the same parameters used for computing the mean zonal wind are shown in Table 1. These values produced by the symmetrical circulation are greater than those inferred from observations, which are of the order of  $25^{\circ}\text{C}$  to  $30^{\circ}\text{C}$ . Since the symmetrical regime is not efficient in transporting heat from equator to pole, a symmetrical regime is no longer stable and a wave regime is bound to develop for the Martian equinoctial seasons. The wave regime, being more efficient in transporting heat from equator to pole, is able to reduce the pole-to-equator temperature difference to the observed value of  $\sim 25^{\circ}\text{C}$  to  $30^{\circ}\text{C}$ .



TABLE 1

THE CALCULATED POLE-TO-EQUATOR TEMPERATURE DIFFERENCES,  
 $T_{pe}$ , AT THE MIDDLE OF THE MARTIAN ATMOSPHERE FOR ASSUMED  
 $A = 10^{10} \text{ cm}^2 \text{ sec}^{-1}$  AND  $\mu = 50, 100, \text{ and } 200 \text{ gm cm}^{-1} \text{ sec}^{-1}$ .

A ( $\text{cm}^2/\text{sec}$ )	$\mu$ ( $\text{gm cm}^{-1} \text{ sec}^{-1}$ )	$T_{pe}$ ( $^{\circ}\text{C}$ )
$10^{10}$	50	53
$10^{10}$	100	49
$10^{10}$	200	44

## SECTION 4

### INTERHEMISPHERIC TRANSPORT OF WATER VAPOR AND THE MARTIAN ICE CAPS

Investigation of the transport of water vapor across Mars by large-scale atmospheric diffusion is being continued. This investigation consists of the development of diffusion models where, with prescribed sources (sublimating polar caps), sinks (forming polar caps), and large-scale diffusion coefficients, latitudinal distributions of water vapor as functions of time can be obtained. Thus, with the above prescribed conditions it is possible to measure the amount of water being transported across the planet, thereby determining the plausibility of the hypothesis that large-scale eddy diffusion of water vapor from the melting polar cap to the forming polar cap can explain the formation of polar caps on Mars despite the low atmospheric water vapor content.

Two models have been developed and are described in Quarterly Progress Reports 1 and 2. Both models include only the source (sublimating polar cap) and not the sink (forming polar cap). In the second of these models, a polar ice cap, initially one centimeter thick and extending from  $60^{\circ}\text{N}$  latitude to the pole, sublimates at a constant rate for 12 terrestrial months. Sublimation occurs only along the perimeter of the cap, and thus the cap recedes toward the pole at the end of the twelfth month. The results of this model are values of water vapor

abundance as a function of latitude and time (time being measured from the start of the sublimation process) for different assumed large scale eddy diffusion coefficients,  $K$ . We are currently attempting to analyze these results in terms of the speed of southward propagation along the Martian surface of a constant value, or isopleth, of water vapor abundance. These speeds of propagation, for different isopleth values and values of  $K$  will be compared to the observed value of the southward speed of propagation ( $\sim 30$  km/day) of the "wave of darkening." In the literature, it has been suggested a number of times that the wave of darkening is a result of the release and subsequent meridional transport of the water vapor from the melting polar cap. With such comparisons, it should be possible to obtain a value of  $K$  that leads to a southward propagation of water vapor that matches the observed speed of the wave of darkening. Deduction of the value of the large scale eddy diffusion coefficient on Mars has important implications for studies of the general circulation and latitudinal heat transfer processes on Mars.

In addition to the work described above, attempts are still being made to develop a more realistic diffusion model in which the effect of a sink for water vapor at the opposite pole is included.

SECTION 5  
ADMINISTRATIVE NOTES

The total number of working hours available during the past quarter totaled 492 hours. The list below indicates the number of hours worked on the project by GCA scientific personnel.

Dr. George Ohring	41
Dr. Wen Tang	284
Dr. Fred House	24
Mr. Joseph Mariano	492
Mr. Richard Harrison	179

## REFERENCES

- Adem, J., 1963: On the theory of the general circulation of the atmosphere. Tellus, 14, 102-115.
- Gandii, L. S., 1955: Osnovy Dinamicheskoi Meteorologii. Gidrometeoizdat, Leningrad, 716 pp. (Chinese Translation edition, 1958).
- Gifford, F. A., Jr., 1964: A study of Martian yellow clouds that display movement. Monthly Weather Review, 92, 425-440.
- Kliore, A., Cain, D.L., Levy, G.S., Eshleman, Von R., Fjeldbo, G., and F.D. Drake, 1965: Occultation experiment: Results of the first direct measurement of Mars' atmosphere and ionosphere. Science, 49, 1243-1248.
- Tang, W., 1965: Some aspects of the atmospheric circulation on Mars. NASA Contract Report NASA CR-262. Prepared under Contract No. NASw-975 by GCA Corporation, Bedford, Mass., 43 pp.